ISBN: 978-3-95450-234-9 ISSN: 2673-5504 doi:10.18429/JACoW-SRF2023-MOPMB008

IN-SITU QUALITY FACTOR MEASUREMENTS OF SRF CAVITIES AT S-DALINAC*

M. Arnold, A. Brauch, M. Dutine, R. Grewe†, L. Jürgensen, N. Pietralla, F. Schließmann, D. Schneider, Institute for Nuclear Physics, Technische Universität Darmstadt, Darmstadt, Germany

Abstract

The Superconducting Darmstadt Linear Accelerator (S-DALINAC) is a thrice recirculating electron accelerator wich can be operated in a multi-turn energy recovery mode. The design parameters for kinetic energy and beam current are up to 130 MeV and up to 20 µA respectively. The injector consists of a six-cell capture cavity and two 20-cell srf cavities. The main linac consists of eight 20-cell cavities. The cavities are operated at a temperature of 2 K with a frequency of 2.9972(1) GHz. Monitoring of the srf cavities is important for the overall performance of the accelerator. A key parameter for the rating of the srf cavity performance is the intrinsic quality factor Q. At the S-DALINAC it is measured for selected cavities during the yearly maintenance procedures. The unique design of the rf input coupler allows for a wide tuning range for the input coupling strength. This makes in-situ quality factor measurements using the decay time measurement method possible. The contribution illustrates the principal design of the input couplers and the benefits it yields for Q measurements. Recent results including the progression of the quality factors over time will be presented.

INTRODUCTION

The thrice recirculating S-DALINAC (Superconducting Darmstadt Linear Accelerator) is in operation since 1991 (Fig. 1). To reach its design energy of 130 MeV within the limited space available at the Institute for Nuclear Physics at TU Darmstadt, the S-DALINAC utilizes the high energy gain and low power losses of superconducting radio-frequency (srf) cavities [1]. At the time the S-DALINAC has been built, 3 GHz 20-cell cavities where figured to be the best compromise of size, dissipated power P_d and accelerating field gradient E_{acc} [2]. Measurement of the performance parameters *intrinsic quality factor* Q_0 and *maximum accelerating gradient* E_{max} of each cavity allows optimization of the energy gain distribution by Q_0, and thus maximizing the total energy gain of the accelerator with respect to total loss $\sum P_d$.

S-DALINAC CRYOMODULES AND INPUT COUPLER

The 20-cell srf cavities of the S-DALINAC are mounted in a frequency tuning frame resting in a liquid helium bath at a temperature of 2 K. A schematic view of the important parts of the S-DALINAC cryomodule is shown in Fig. 2.

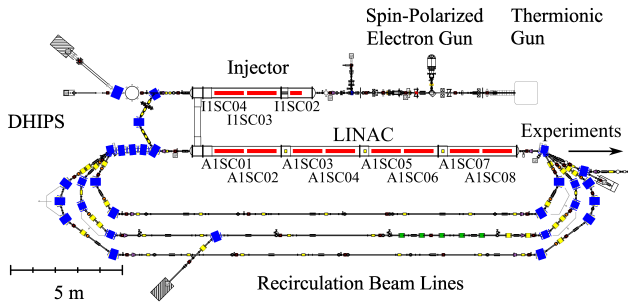

Figure 1: Floorplan of the S-DALINAC accelerator hall. Two electron sources create an electron current of up to 60 µA with an energy of up to 250 keV which is prepared for srf acceleration in a normalconducting section. A single 5-cell cavity and two 20-cell cavities (red) are used to capture and accelerate the beam to 10 MeV to be used for nuclear fluorescence experiments or further acceleration in the main LINAC. The main LINAC consists of eight 20-cell cavities, which add up to 30 MeV to the beam energy in each of up to four passes.

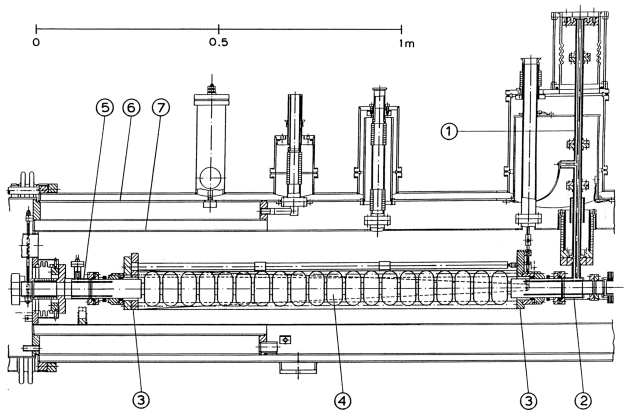

Figure 2: Sectional view of a cut in half cryomodule of the S-DALINAC . (1) Coaxial rf transmission line, (2) Coaxial input coupler, (3) Cavity tuning frame, (4) 20-cell elliptical cavity, (5) rf output coupler, (6) 80 K shielding, (7) 2 K helium vessel [3].

To optimize the operation of the Low Level RF control (LLRF) [4] for each cavity, the rf transmission line allows variation of the penetration depth of the rf input antenna into the coaxial input coupler by means of a bellow in the outer conductor of the transmission line. A detailed schematic of the input coupler layout is shown in Fig. 3. By variation of the penetration depth the external quality factor Q_{ex} can be adjusted in the range $3 \cdot 10^6 < Q_{ex} < 3 \cdot 10^9$ [3], covering the design quality factor $Q_0 = 3 \cdot 10^9$ of the srf cavities.

* Work supported by DFG (GRK 2128) and the State of Hesse within the Research Cluster ELEMENTS (Project ID 500/10.006)
† rgrewe@ikp.tu-darmstadt.de

ISBN: 978-3-95450-234-9 ISSN: 2673-5504 doi:10.18429/JACoW-SRF2023-MOPMB008

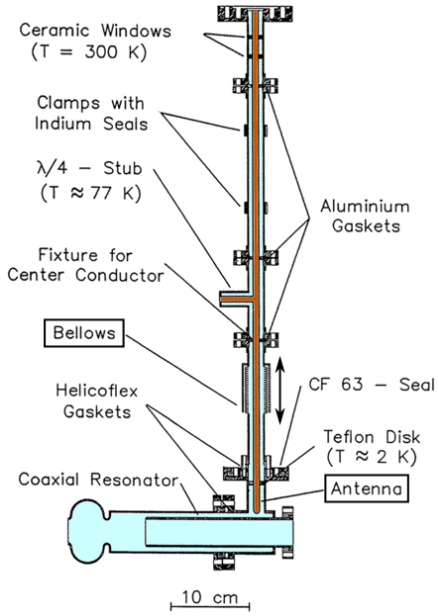

Figure 3: Schematic sectional detail view of the S-DALINAC input coupler. The bellows allow for a large coupling strength adjustment range by vertical change of the penetration depth of the input antenna, enabling a critical coupling with $\beta = 1$ to the cavity [3].

Allowing a large variation of Q_{ex}, the rf input transmission line of the S-DALINAC cryomodules offer the potential of establishing an *in-situ quality factor measurement* using a decay time measurement method, which is often used for Q_0 measurement during pre-installation testing of srf cavities in vertical bath cryostats [5–8]. With this measurement principle, a performance monitoring of the srf cavities of the S-DALINAC with minimal uncertainties is performable.

MEASUREMENT SETUP

The uncertainty for a measurement of the intrinsic quality factor Q_0 of the cavity has a strong dependency on the external quality factor Q_{ex} of the input coupler as shown in Ref. [9]. By defining the coupling strength β as the ratio:

$$\beta = \frac{Q_{ex}}{Q_0},$$

it is feasable to have a value of $\beta < 5$ for satisfactory small uncertainties.

For electron acceleration operation the srf cavities are operated with a sophisticated, in-house developed LLRF control hardware [10] to control frequency and phase. The LLRF requires a minimal π-mode resonance width (FWHM) of $\Delta f > 100$ Hz. Typical coupling strengths required to achieve this width are $\beta > 10$, implying the constraint for low δQ_0 is not fullfilled by the requirements of the LLRF hardware. On the other hand, for measuring Q_0 the value and relation of phase and frequency is dispensable. It is sufficient to have the rf input power frequency locked to the resonance frequency f_0 of the cavity. Therefore, a phase locked-loop (PLL) [11] is the central element of the decay time Q_0 measurement set-up. The principle set-up as shown in Fig. 4 is based on the detailed description in Ref [9]. The PLL consists of (1) a rf mixer and a 10 kHz low pass-filter (LPF) generating a DC voltage signal proportional to the frequency difference of the cavity resonance and signal generator output, (2) the signal generator using the DC voltage signal to vary its output frequency, and (3) a phase shifter to match the PLLs signal propogation time to the propogation time of the rf signal through the cavity. The signal generator rf output is split by a 6 dB directional coupler, the main part is used to drive the cavity through an rf amplifier. For measurement of the forward and reverse rf powers, a bidirectional coupler close to the cavity is used. Schottky diodes or rf measurement boards made in-house [12] convert the rf signal to a dc voltage, which is recorded with an oscilloscope. The operation of the rf mixer needs power levels between 0 – 10 dBm at the RF and LO inputs, ensured by using fixed or variable rf attenuators prior to these inputs. Additionally, the components of the set-up might be used by other experiments, making an open, table-top set-up best suited. In Fig. 5 a photograph of the PLL set-up is shown.

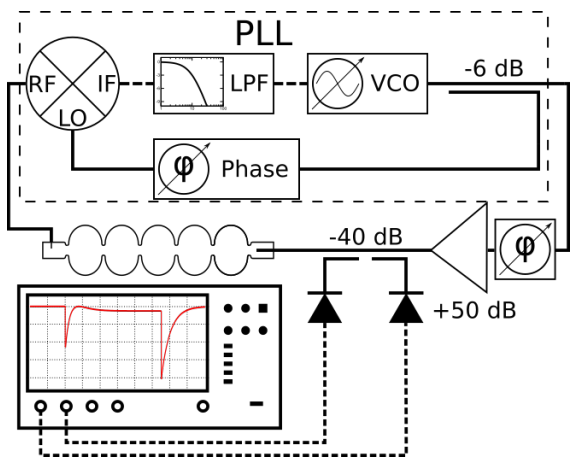

Figure 4: Schematic of the measurement set-up. A phased-lock-loop (PLL) is used to track the resonance frequency f_0 of the cavity. Depending on the coupling strength β an main rf amplifier outputs up to 100 W to reach quenching fields. Schottky diodes or rf measurement boards made in-house connected to the ports of a bidirectional coupler convert the forward P_f and reverse P_r rf powers to a DC voltage. The voltage is recorded using an oscilloscope.

MEASUREMENT METHOD

The coupling strength β is adjusted as near as possible to critical coupling $\beta = 1$ using a vector network analyzer (vna) or the PLL set-up presented. Using the PLL with a pulsed rf forward power the measured reverse power has a distinct shape depending on the coupling strength [13]. For a precise measurement, one has to take into account the dampening factor of the rf transmission lines between the directional coupler and the cavity input coupler. This is

ISBN: 978-3-95450-234-9 ISSN: 2673-5504 doi:10.18429/JACoW-SRF2023-MOPMB008

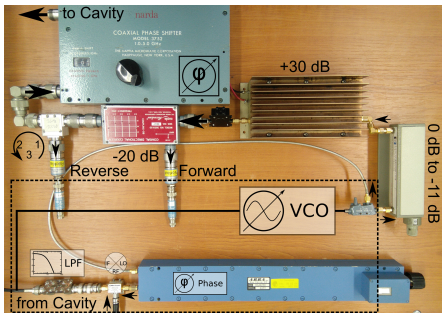

Figure 5: Photograph of the set-up used for Q vs. E measurement.

accomplished by a *off-resonance measurement*. In our case, the output frequency is modulated by a depth of $f_0 \pm$ 4 MHz with a modulation frequency of 10 Hz. The forward rf power P_f and reverse rf power P_r at the cavity is then given by:

$$\begin{aligned} P_\mathrm{f} &= (k_\mathrm{r} \cdot k_\mathrm{f})^{-1/2} \cdot \sqrt{P_\mathrm{r}^\mathrm{off}/P_\mathrm{f}^\mathrm{off}} \cdot P_\mathrm{f}^\mathrm{m} \\ P_\mathrm{r} &= (k_\mathrm{r} \cdot k_\mathrm{f})^{-1/2} \cdot \sqrt{P_\mathrm{f}^\mathrm{off}/P_\mathrm{r}^\mathrm{off}} \cdot P_\mathrm{r}^\mathrm{m} \end{aligned} \tag{1}$$

using the coupling coefficients of the bidirectional coupler $k_\mathrm{r,f}$, the average off resonance powers measured at the ports of the bidirectional couplers $P_\mathrm{r,f}^\mathrm{off}$ and the measured powers during the decay time measurement $P_\mathrm{r,f}^\mathrm{m}$. For a pulsed forward power and applied *off-resonance* correction the forward and reverse powers are shown in Fig. 6. The quality factor Q_0 is calculated using the decay time τ, coupling strength β and resonance frequency f_0:

$$Q_0 = (1 + \beta) \cdot 2\pi f_0 \cdot \tau. \tag{2}$$

The coupling strength β is calculated by

$$\begin{aligned} \beta_\mathrm{fre} &= \frac{P_\mathrm{e}}{P_\mathrm{f} - P_\mathrm{r}} \\ \beta_\mathrm{fr} &= \frac{1 \pm \sqrt{P_\mathrm{r}/P_\mathrm{f}}}{1 \mp \sqrt{P_\mathrm{r}/P_\mathrm{f}}} \\ \beta_\mathrm{fe} &= \frac{1}{2 \cdot \sqrt{P_\mathrm{f}/P_\mathrm{e}} - 1} \\ \beta &= 1/3 \cdot (\beta_\mathrm{fre} + \beta_\mathrm{fr} + \beta_\mathrm{fe}) \end{aligned} \tag{3}$$

using the equilibrium powers P_r, P_f and P_e, as indicated in Fig. 6.

For high field gradients effects like multipacting or field emission of electrons have to be taken into account. The discussed quality factor measurement is only accurate for low electromagnetic fields not affected by these effects. For high fields the proportionality between the output power P_t and the stored energy U is utilized:

$$U = \frac{Q_0 P_\mathrm{d}}{2\pi f_0} = \kappa P_\mathrm{t}$$

The propotionality constant κ is measured by a low-field decay time quality factor measurement and the dissipated power is given by:

$$P_\mathrm{d} = P_\mathrm{f} - P_\mathrm{r}$$

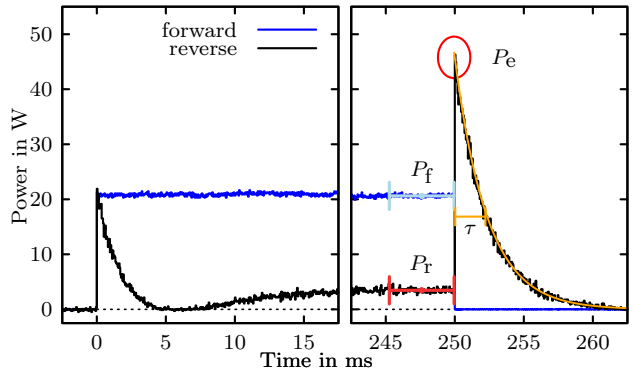

Figure 6: A rectangular pulse in forward power (blue) is feed to the cavity. The equilibrium powers and the decay time is derived as indicated from the pulse responce of the cavity.

For high fields it is sufficient to measure the forward, reverse and through powers P_f, P_r, P_t. The accelerating field E_acc and the quality factor $Q_0$are then obtained by:

$$\begin{aligned} E_\mathrm{acc} &= \sqrt{R/Q\omega_0 \cdot U} \cdot l^{-1} \\ Q_0 &= \frac{(1+\beta)^2\,\omega_0}{4\beta^2 P_\mathrm{f}} \cdot U. \end{aligned}$$

To assist the researcher in charge of the measurement, a software has been implemented to collect and store all relevant data and automate the process of the calculation of Q_0 and E_acc using the methods described. The uncertainty calculation involves many equations wich are not given in this paper. A comprehensive collection of equations for calculation of the unloaded quality factor using different methods are given in e.g. Ref. [9] or [13].

RESULTS

The first measurement using the decay time method *in-situ* has been conducted in 2015 with low accelerating fields. In the following years the measurement has been repeated with accelerating fields up to the quenching limit. Out of time constraints we were not able to measure all cavities in every year. In Fig. 7 the highest Q_0 reached for each cavity for selected years is pictured, and in Fig. 8 the maximum for acceleration usable field gradient E_acc is shown. The unloaded quality factor of many cavities seems to fluctuate more (A1SC05, A1SC06, I1SC03) or less (A1SC01, A1SC03, A1SC04, A1SC07, A1SC08) around a value. We need further investigation to clarify the fluctuations. They might be introduced by differences in the cooldown process, moving particles on the surface or some other process. These effects are not easy to investigate, though. Cavity A1SC02 has been cleaned in an ultrasonic bath at DESY, Hamburg, in 2018, which at least explains the higher Q_0 and E_acc values since 2018. A cleaning of cavities A1SC07, A1SC08, I1SC01, I1SC02 and I1SC03 might yield gains simliar to A1SC02, to around $1 \cdot 10^9$.

ISBN: 978-3-95450-234-9 ISSN: 2673-5504 doi:10.18429/JACoW-SRF2023-MOPMB008

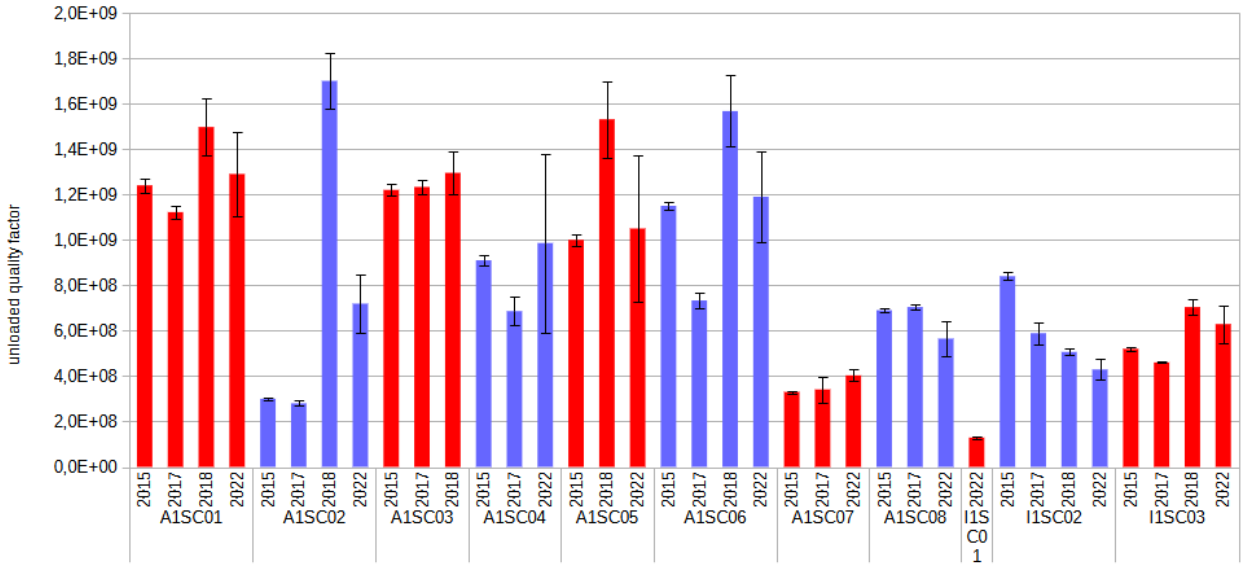

Figure 7: Comparison of Q_0 measurements for different years. A1SC0* denotes linac cavities, I1SC0* injector cavities.

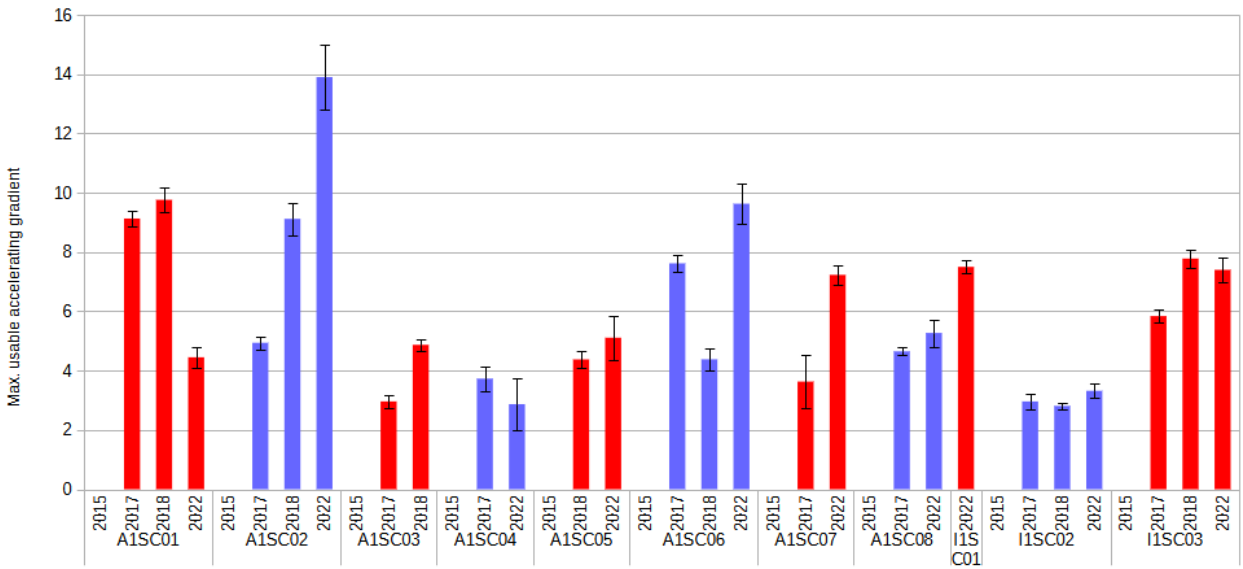

Figure 8: Comparison of E_{acc} measurements for different years. A1SC0* denotes linac cavities, I1SC0* injector cavities. The measurement in 2015 comprised only measuerements at low accelerating fields and is thus empty in this plot.

SUMMARY AND OUTLOOK

The quality factor measurement at the S-DALINAC is performed using components that were available, with as little as possible complexity. Still the results are very useful for everyday beam tuning of the accelerator and to identify problematic cases of too low performance. It might be possible to increase the performance of cavities by using relativly simple ultrasonic cleaning, but the deassambly and assembly processes are risky. A cavity that is going to be cleaned during the next possible maintenance phase is the first injector cavity I1SC01.

Because of related costs and manpower needed, it is not feasible to try to increase all quality factors - it might not even be possible to increase Q_0 much over $1 \cdot 10^9$ for installed cavities. But the measurement of the quality factors of all cavities yields the possibility to optimize the overall dissipated energy by distributing the energy gain of each cavity according to its Q_0. This leads to more headroom for the liquid helium cryoplant of the S-DALINAC and/or higher achievable field gradients, depending on the experimental setup.

REFERENCES

[1] F. Schliessmann *et al.*, "Realization of a multi-turn energy recovery accelerator", *Nat. Phys.*, 2023. doi:10.1038/s41567-022-01856-w

ISBN: 978-3-95450-234-9 ISSN: 2673-5504 doi:10.18429/JACoW-SRF2023-MOPMB008

[2] T. Grundey *et al.*, "Construction and first operation of a pilot cw superconducting electron accelerator", *Nucl. Instrum. Methods Phys. Res., Sect. A*, vol. 224, no. 1, pp. 5–16, 1984. doi:10.1016/0167-5087(84)90442-3

[3] T. Rietdorf, "Entwurf und Realisierung einer variablen supraleitenden Hochfrequenz-Einkopplung für die Beschleunigerstrukturen des supraleitenden Darmstädter Elektronenbeschleunigers S-DALINAC", D17, Dissertation, Technische Hochschule Darmstadt, 1993.

[4] M. Konrad *et al.*, "Digital base-band rf control system for the superconducting Darmstadt electron linear accelerator" ,*Phys. Rev. Spec. Top. Accel. Beams*, vol. 15, p. 052 802, 2012. doi:10.1103/PhysRevSTAB.15.052802

[5] J. P. Holzbauer, B. M. Hanna, Y. M. Pischalnikov, W. Schappert, D. A. Sergatskov, and A. I. Sukhanov, "Precision Q0 Measurement of an SRF Cavity with a Digital RF Techniques", in *Proc. IPAC'18*, Vancouver, Canada, Apr.-May 2018, pp. 2674–2677. doi:10.18429/JACoW-IPAC2018-WEPML003

[6] D. Reschke *et al.*, "Performance in the vertical test of the 832 nine-cell 1.3 GHz cavities for the european x-ray free electron laser", *Phys. Rev. Accel. Beams*, vol. 20, p. 042 004, 2017. doi:10.1103/PhysRevAccelBeams.20.042004

[7] V. A. Goryashko *et al.*, "High-Precision Measurements of the Quality Factor of Superconducting Cavities at the FREIA Laboratory", in *Proc. SRF'15*, Whistler, Canada, Sep. 2015, pp. 810–813. https://jacow.org/SRF2015/papers/TUPB089.pdf

[8] H. Piel, "Diagnostic Methods of Superconducting Cavities and Identification of Phenomena", in *Proc. SRF'80*, Karlsruhe, Germany, Jul. 1980. https://jacow.org/srf80/papers/SRF80-5.pdf

[9] T. Powers, "Theory and Practice of Cavity RF Test Systems", in *Proc. SRF'05*, Ithaca, NY, USA, Jul. 2005, pp. 40–70. https://jacow.org/SRF2005/papers/SUP02.pdf

[10] M. Konrad, "Development and comissioning of a digital rf control system for the S-DALINAC and migration of the accelerator control system to an EPICS-based system", D17, Dissertation, Technische Universität Darmstadt, 2013.

[11] F. M. Gardner, *Phaselock Techniques*. Wiley-Interscience, 2005.

[12] M. Steinhorst *et al.*, "Rf average power measurement system at the S-DALINAC", *Nucl. Instrum. Methods Phys. Res., Sect. A*, vol. 1010, p. 165 567, 2021. doi:10.1016/j.nima.2021.165567

[13] H. Padamsee, J. Knobloch, and T. Hays, *RF Superconductivity for Accelerators*, 2nd ed. Wiley-VCH, 2007.